An improved model for hydrate formation in sulfuric acid–water nucleation

M. Noppel
Institute of Environmental Physics, University of Tartu, 18 Ülikooli Str. 50090 Tartu, Estonia and Department of Physics, P.O. Box 64, 00014 University of Helsinki, Finland

H. Vehkamäki[a] and M. Kulmala
Department of Physics, P.O. Box 64, 00014 University of Helsinki, Finland

(Received 12 July 2001; accepted 5 October 2001)

The formation of sulfuric acid–water hydrates in the vapor phase and nucleation rates of sulfuric acid–water clusters are investigated. The result of *ab initio* calculations and experimental data related to hydrates are utilized to improve the description of sulfuric acid–water hydration and nucleation in atmospheric conditions. The nucleation rates are obtained using the most rigorous nucleation kinetics and the thermodynamically consistent version of the classical nucleation model. The improvements increase the predicted nucleation rates compared to previous models. The predicted nucleation rates are compared with experimental ones, and they are in most cases within experimental errors. Some experimental evidence suggests that the present model gives a more realistic dependence of nucleation rate on relative humidity and sulfuric acid concentration than the earlier versions of the theory. © *2002 American Institute of Physics.* [DOI: 10.1063/1.1423333]

I. INTRODUCTION

Formation of atmospheric aerosols has recently received growing experimental and theoretical interest due to climate and health related effects of fine particles.[1,2] The increased aerosol concentrations are largely due to secondary particle production, i.e., homogeneous nucleation from vapors. Instrument techniques for measuring freshly formed particle concentrations have been recently developed, and particles with a diameter of about 3 nm can be detected. These small particles have been found in the free troposphere,[3–5] in the marine boundary layer,[6–8] in the vicinity of evaporating clouds,[9] in Arctic areas,[10,11] in urban areas and in stack plumes,[12] and recently also in forests.[13–15]

Although new theoretical approaches[16] using, for example, *ab initio* molecular dynamics[17] and Monte Carlo simulations[18] have been developed, the classical nucleation theory[19] is still the only one which can be used in atmospheric applications, particularly in atmospheric models. It is important to make sure that the classical predictions are made using thermodynamically consistent theories and therefore detailed thermodynamics is needed.[20,21] However, molecular approaches are needed to confirm the results obtained by classical theories and in future, hopefully, parameterized versions of molecular models could be used in atmospheric models.

The classical theory of binary homogeneous nucleation was first treated in the 1930's by Flood,[22] but it was not until almost 20 years later that Reiss[23] published a complete treatment of binary nucleation. Doyle[24] was the first to publish predicted nucleation rates for the sulfuric acid/water system. A free sulfuric acid molecule tends to gather water molecules around it to form hydrates. Heist and Reiss[25] and Jaecker-Voirol *et al.*[26] improved the classical theory taking into account the effect of sulfuric acid hydration. The hydrates stabilize the vapor and reduce the nucleation rates by a factor 10^3-10^8. Recently Noppel[27] developed the hydrate model further. Wilemski[28] presented a revised classical nucleation theory, and pointed out that the previous standard nucleation theory was thermodynamically inconsistent. Namely, the numerical method to search the critical cluster (a smallest thermodynamically stable cluster) was not correct, and it resulted in wrong cluster composition and nucleation rates.[29] Kulmala *et al.*[30] have performed parameterizations for the nucleation rate as a function of temperature, relative humidity and acidity using thermodynamically consistent theory. However, they used some approximations in nucleation kinetics and an old model for the hydrates.

The prediction of binary nucleation theory that small quantities of sulfuric acid would significantly enhance the water vapor nucleation has been verified experimentally. For example Viisanen *et al.*[31] carried out quantitative experiments at 298 K using a steady flow reactor with 38% and 52% relative humidity. Their results were in reasonable agreement with previous more qualitative experiments[32,33] and with the binary theory where hydrates were included.[30] Also a recent experimental study by Ball *et al.*[34] agrees qualitatively with theoretical predictions. It should be noted that these laboratory studies have all been done at sulfuric acid vapor concentrations that are much higher than values measured in the atmosphere. The latter ones have seldom exceeded 10^8 molecules/cm^3, even when nucleation is observed.[35] Nucleation at low sulfuric acid concentrations may be explained partly by the low temperatures encountered during many of the reported atmospheric studies and by the possible participation of other species like ammonia in atmospheric nucleation processes.[36,37]

One of the main difficulties for predicting the nucleation rate of sulfuric acid–water vapor, compared with other binary systems, arises from the tendency of sulfuric acid to

[a]Author to whom correspondence should be addresssed.

form hydrates (small clusters of acid and water molecules) in the gas phase.[26,27] Since the formation energy of hydrates is negative, it is energetically more difficult to form critical nuclei out of sulfuric acid hydrates than from free acid molecules. In practice the total sulfuric acid concentration is measured both in laboratory and atmospheric experiments. On the other hand, the concentration of free, unbound acid molecules is needed in order to calculate the formation free energy of a critical nucleus and the nucleation rate. The relation between total and free acid concentrations is usually obtained using capillarity approximation;[26] the tiny hydrates containing one to ten water molecules and one sulfuric acid molecule are incorrectly treated using the surface tension and density of a macroscopic liquid. McGraw and Weber[38] compared the results of total acid measurements of Marti *et al.*[39] with the predictions of classical liquid drop model and showed that the model overestimates the extent of hydrate formation. Since the effect of hydrate formation is significant, a more accurate way to describe hydrates should be found. In the present study we have used the result of *ab initio* calculations as well as experimental data related to hydrates to improve the description of sulfuric acid–water nucleation in atmospheric conditions.

First we summarize the classical droplet model (Sec. II), then the hydrate formation is described (Sec. III). In Sec. IV the fitting procedure used to improve the hydrate interaction model is presented. The self-consistent equilibrium binary distribution is described in Sec. V. The procedures to calculate the formation work of a critical cluster (Sec. VI) and nucleation rate (Sec. VII) including detailed multicomponent kinetics are summarized after that. Finally in Sec. VIII we present results including comparisons with laboratory experiments[31,34,40] and the parameterization by Kulmala *et al.*[30]

II. CLASSICAL DROPLET MODEL

A cluster containing n_a and n_w molecules of acid and water, respectively, is described as a spherical liquid droplet and the Gibbsian formulation of Nishioka *et al.*[41] is adopted. The radius of the Gibbs dividing surface is r and it encompasses a volume V of uniform liquid. Let ρ_{il} be the number density of species i in the uniform liquid. The total number of molecules of species i is expressed as $n_i = n_{il} + n_{is}$, where the number of molecules in the bulk phase is $n_{il} = \rho_{il}(x)V$,

$$x = n_{al}/(n_{al}+n_{wl}) \tag{1}$$

is the mole fraction of acid in the interior "core" of the cluster and n_{is} is the surface excess number of molecules that corrects for the difference between the density profiles of our uniform droplet model and the actual cluster. The surface tension γ of clusters does not depend on their radius if and only if the equimolar surface given by the condition[42,43]

$$n_{as}v_a(x) + n_{ws}v_w(x) = 0 \tag{2}$$

coincides with the surface of tension. Here v_w denotes the partial molecular volume of water and v_a is the partial molecular volume of sulfuric acid.

We fix the the Gibbs dividing surface at the surface of tension and assume curvature independent surface tension. The volume of the cluster is now given by

$$V = \frac{4\pi}{3}r^3 = n_a v_a(x) + n_w v_w(x) = n_{al}v_a(x) + n_{wl}v_w(x), \tag{3}$$

and the molecular numbers in the core of the cluster by

$$n_{al} = \frac{4\pi r^3 x/3}{x v_a(x) + (1-x)v_w(x)}, \tag{4}$$

$$n_{wl} = \frac{4\pi r^3 (1-x)/3}{x v_a(x) + (1-x)v_w(x)}. \tag{5}$$

The Gibbs adsorption isotherm[41]

$$n_{as}d\mu_{al} + n_{ws}d\mu_{wl} + 4\pi r^2 d\gamma = 0 \tag{6}$$

together with Eq. (2) leads to the following expressions for the surface excess numbers:[42,43]

$$n_{as} = \frac{4\pi r^2 \dfrac{d\gamma}{dx}}{\dfrac{v_a}{v_w}\dfrac{d\mu_{wl}}{dx} - \dfrac{d\mu_{al}}{dx}}, \tag{7}$$

$$n_{ws} = \frac{4\pi r^2 \dfrac{d\gamma}{dx}}{\dfrac{v_w}{v_a}\dfrac{d\mu_{al}}{dx} - \dfrac{d\mu_{wl}}{dx}}. \tag{8}$$

Here $\mu_{al} = \mu_{al}(p_l, x)$ and $\mu_{wl} = \mu_{wl}(p_l, x)$ are the chemical potentials of sulfuric acid and water, respectively, in the uniform liquid core with mole fraction x. p_l is the liquid pressure in the interior of the cluster. The derivatives are taken with fixed cluster radius r and vapor properties [$\mu_{iv}(p_v)$ and ρ_i^{free} below]. The chemical potential in the liquid is related to the chemical potential in the vapor μ_{iv} by equation

$$\mu_{il}(p_l, x) = \mu_{iv}(p_v) - kT \ln \frac{\rho_i^{\text{free}}}{\rho_{i,s}^{\text{free}}(x)} + \frac{2v_i(x)\gamma(x)}{r}, \tag{9}$$

where p_v is the vapor pressure, ρ_i^{free} is the concentration of free molecules of component i in the vapor. $\rho_{i,s}^{\text{free}}(x)$ is the concentration of free molecules of component i in the equilibrium vapor above a flat surface of a solution which has the acid mole fraction x. Here we have, as usual, omitted the numerically negligible terms $v_i(p_v' - p_s)$, where p_v' is the total pressure of a vapor where the cluster would be critical, and p_s is the total pressure in the equilibrium vapor.

If the liquid in the cluster is assumed incompressible the formation free energy of the cluster can be written as[44]

$$\begin{aligned}\Delta G(n_a, n_w) = {} & (\mu_{al}(p_v) - \mu_{av})n_{al} + (\mu_{wl}(p_v) - \mu_{wv})n_{wl} \\ & + (\mu_{as} - \mu_{av})n_{as} + (\mu_{ws} - \mu_{wv})n_{ws} \\ & + 4\pi r^2 \gamma.\end{aligned} \tag{10}$$

Here $\mu_{il}(p_v)$ is the chemical potential of component i in the liquid at the vapor pressure and μ_{as} is the chemical potential of the surface phase.

We assume the vapor surrounding the cluster ideal and the chemical potential of the surface phase equal to the chemical potential in the liquid $\mu_{is}=\mu_{il}(p_l,x)$, and use Eqs. (2) and (9) to express the chemical potentials in terms of vapor concentrations. If we neglect again the small terms $v_i(p_v-p_s)$, the formation work of the cluster can be expressed as[43]

$$\Delta G(n_a,n_w)=-n_a kT\ln(\rho_a^{\text{free}}/\rho_{a,s}^{\text{free}}(x)) - n_w kT\ln(\rho_w^{\text{free}}/\rho_{w,s}^{\text{free}}(x))+4\pi r^2\gamma. \quad (11)$$

III. HYDRATE FORMATION

The concentration of hydrate (clusters containing one sulfuric acid and i water molecules) is given by [45]

$$\rho(1,i)=K_1\cdot K_2\cdot\cdots\cdot K_i\left(\frac{\rho_w^{\text{free}}}{\rho_0}\right)^i\rho_a^{\text{free}}, \quad (12)$$

where K_i are the equilibrium constants for the successive additions of water molecules to an acid molecule, ρ_a^{free} and ρ_w^{free} are the vapor phase concentrations of free acid and water molecules, respectively. The equilibrium constants are calculated at the reference vapor concentration $\rho_0=p_0/(kT)$. The arbitrary reference pressure p_0 is usually taken to be 1 atm. Here k is the Boltzmann constant and T is the absolute temperature. Throughout this work we use the usual assumption that the concentration of sulfuric acid is much lower than that of water so that the concentration of water is not significantly affected by the hydrate formation ($\rho_w^{\text{free}}=\rho_w^{\text{total}}$), and ignore the concentrations of hydrates with more than one acid molecule. The relation between the free and total acid concentrations in the vapor is given by[26,46]

$$\frac{\rho_a^{\text{total}}}{\rho_a^{\text{free}}}=1+K_1\frac{\rho_w^{\text{free}}}{\rho_0}+\cdots+K_1\cdot K_2\cdot\cdots\cdot K_i\left(\frac{\rho_w^{\text{free}}}{\rho_0}\right)^i+\cdots + K_1\cdot K_2\cdot\cdots\cdot K_N\left(\frac{\rho_w^{\text{free}}}{\rho_0}\right)^N, \quad (13)$$

where N is the number of water molecules in the largest hydrate taken into account. The equilibrium constants can be expressed as

$$\ln K_i=\frac{-\Delta G_i}{RT}=\frac{-(\Delta H_i-T\Delta S_i)}{RT}, \quad (14)$$

where ΔG_i, ΔH_i, and ΔS_i are, respectively, the free energy, the enthalpy, and entropy change per mole of addition of one water molecule to a hydrate with $i-1$ water molecules, and R is the molar gas constant. The classical hydration model formulated by Jaecker-Voirol *et al.*[26] gives the standard free energy of addition of a water molecule to an $(i-1)$ hydrate as

$$\Delta G_i=\frac{\partial\Delta G(1,i)}{\partial i}=-RT\ln\frac{\rho_0}{\rho_{w,s}^{\text{free}}(x)}+\frac{2\gamma(x)v_w(x)N_a}{r}, \quad (15)$$

where N_a is the Avogadro constant. In nucleation calculations the hydrate composition is usually estimated by Doyle's method, i.e., at the average acid mole fraction,

$$x_{\text{ave}}=n_a/(n_a+n_w)=1/(1+i). \quad (16)$$

From the point of view of macroscopic thermodynamics it is more consistent to use the interior bulk mole fraction of a cluster, Eq. (1). For the hydrates we know *a priori* the total molecular numbers, but not the molecular numbers n_{al} and n_{wl} in the core, but they can be solved from Eqs. (4), (7), (5), and (8) keeping in mind that the radius r is related to the total molecular numbers by Eq. (3). It is also more correct not to use the differentiation but to take the difference in deriving the free energy change in water addition,

$$\Delta G_i=\Delta G(1,i)-\Delta G(1,i-1). \quad (17)$$

The hydration enthalpies, entropies, free energies and equilibrium constants calculated by different levels of approximations in the classical liquid drop model are presented in the first six rows of Table I. The results obtained using water and acid activities by Zeleznik[47] and Clegg and Brimblecombe[48] are compared. Throughout this work we use the liquid density and surface tension given by Myhre *et al.*[49] The enthalpies of hydration are calculated by the Gibbs–Helmholtz equation,

$$\Delta H_i=\frac{\partial(\Delta G_i/T)}{\partial(1/T)}. \quad (18)$$

The entropies ΔS_i are obtained using Eq. (14), where ΔG_i are estimated by Eq. (15) or (17) and ΔH_i is calculated by Eq. (18).

The values calculated by different versions of the liquid drop model in Table I show rather large divergence. Equilibrium constants for monohydrate differ by a factor 6.8 and constants for dihydrate by a factor 2.6. We see that in the scope of a liquid drop model the values of equilibrium constants K_1 and K_2 depend essentially on the approximation used and, accordingly, the calculated nucleation rate values can differ more than 4–7 orders of magnitude.[46,50] More reliable values for equilibrium constants K_1 and K_2 are clearly required.

The next 10 rows of Table I list the results of *ab initio* calculations presented in the literature. Again the divergence of equilibrium constant values is large, but in the values of entropy the divergence is rather small, only 7.5% for monohydrate and 3% for dihydrate. The experimental values for K_1, K_2 are available only for temperature $T=298$ K (Ref. 51) and they are shown on the last row of Table I. Calculation of free energy (and thus the equilibrium constant) involves subtraction of two close values (ΔH_i and $T\Delta S_i$) and is therefore very sensitive to the accuracy of these values.

IV. FITTING FOR EQUILIBRIUM CONSTANTS

In this paper we follow the procedure proposed by Noppel[27] to obtain the formation enthalpies, entropies, and furthermore the equilibrium constants of the mono- and dihydrates by fitting these values to the data in Table I and the experimental data of sulfuric acid equilibrium vapor pressure.

Marti *et al.*[39] report the pressures $p_a^{\text{total}}=\rho_a^{\text{total}}kT$ corresponding to the total sulfuric acid concentration in the

TABLE I. Gas phase hydration enthalpies ΔH_i, entropies ΔS_i, free energies ΔG_i, and equilibrium constants K_i ($i=1,2$) at $T=298.15$ K. The values on six first rows are calculated by the classical liquid drop model (CLD): ∂ refers to Eq. (15), Δ refers to Eq. (17). x_{core} refers to Eq. (1), x_{ave} refers to Eq. (16). Also the activities used (Zeleznik or Clegg *et al.*) in the calculation are indicated. Next ten rows are results of *ab initio* calculations. The rows marked with D95 are all B3LYP results taken from Re *et al.* (Ref. 64), different values correspond to different basis sets [(D95(d,p) and D95++(d,p)] and different structure (I-n, etc.). The last row shows experimental results.

ΔH_1 kJ/mol	ΔS_1 J/mol K	ΔG_1 kJ/mol	K_1[a]	ΔH_2 kJ/mol	ΔS_2 J/mol K	ΔG_2 kJ/mol	K_2[a]	Reference
−57.0	−128	−18.8	1950	−48.0	−128	−9.9	55.3	CLD, ∂, x_{ave}, Zeleznik[d]
−66.9	−177	−14.0	287	−44.2	−120	−8.4	29.2	CLD, ∂, x_{core}, Zeleznik[d]
−62.2	−153	−16.5	777	−53.6	−144	−10.7	75.7	CLD, Δ, x_{core}, Zeleznik[d]
−36.2	−60.4	−18.2	1520	−36.9	−90.6	−9.9	54.3	CLD, ∂, x_{ave}, Clegg *et al.*[e]
−46.3	−110	−13.4	227	−33.4	−84.0	−8.3	29.0	CLD, ∂, x_{core}, Clegg *et al.*[e]
−33.7	−55.1	−17.3	1060	−38.5	−94.1	−10.5	68.8	CLD, Δ, x_{core}, Clegg *et al.*[e]
−38[b]				−48[b]				Arstila *et al.*[f]
−54.7[c]	−123[c]	−18.0[c]	1450[c]					Beichert *et al.*[g]
−40.6	−128	−2.4	2.6	−38.7	−128	−0.4	1.2	Bandy *et al.*[h55]
−64.8[b]								Kurdi *et al.*[i]
−56.1	−127	−18.2	1520	−55.7	−130	−17.0	946	D95(d,p) I-n, II-n-a
−44.0	−129	−5.5	9.2					D95(d,p) I-c
				−54.4	−132	−15	421	D95(d,p) II-n-b
−46.5	−123	−9.9	54	−47.3	−131	−8.2	28	D95++(d,p) I-n, II-n-a
−36.0	−120	−0.3	1.1					D95++(d,p) I-c
				−44.0	−128	−5.8	10	D95++(d,p) II-n-b
			410				50	Hanson *et al.*[j]
			± 94.5				± 9.45	Experimental error estimates

[a]Equilibrium constants are given for the reference vapor pressure 1 atm.
[b]Evaluated by *ab initio* at $T=0$ K, no zero point vibrational correction.
[c]The enthalpies ΔH_i and entropies ΔS_i are considered to be temperature independent and they are calculated from the values of ΔG_i given by Beichert and Schrems (Ref. 65) for $T=195$ K and $T=230$ K.
[d]Reference 47.
[e]Reference 48.
[f]Reference 17.
[g]Reference 65.
[h]Reference 55.
[i]Reference 66.
[j]Reference 51.

equilibrium vapor above aqueous solutions with sulfuric acid mass fraction $x_{\mathrm{mass}}=0.55-0.77$ (corresponding to about 5%–25% relative humidity) at temperatures 298.15, 303.15, and 308.15 K. Their data consist of 47 points $(p_{a,i}, x_{\mathrm{mass},i})$ (the data point $x_{\mathrm{mass}}=0.541$, $T=298.15$ K was excluded from our analysis due to remarkable deviation from the trend of other points).

The total acid concentrations are related to the free acid concentrations by Eq. (13), and the water concentration in the equilibrium vapor is given by

$$\rho_{w,s}^{\mathrm{free}}(x)=p_{w,s}^{\mathrm{free}}(x)/kT=p_{w,s}^{\mathrm{pure}}A_w(x)/kT, \tag{19}$$

where $A_w(x)$ is the water activity in the solution, and $p_{w,s}^{\mathrm{free}}(x)=p_{w,s}^{\mathrm{total}}(x)$ and $p_{w,s}^{\mathrm{pure}}$ are the equilibrium vapor pressures for the solution and pure water, respectively. The concentration of free acid molecules in the equilibrium vapor is given by

$$\rho_{a,s}^{\mathrm{free}}(x)=p_{a,s}^{\mathrm{free}}(x)/kT=p_{a,s}^{\mathrm{pure}}A_a(x)/kT, \tag{20}$$

where $p_{a,s}^{\mathrm{free}}(x)$ and $p_{a,s}^{\mathrm{pure}}$ are the equilibrium vapor pressures above the solution and pure liquid sulfuric acid, respectively and $A_a(x)$ is the acid activity in the solution.

We compare the results calculated with activities given by Zeleznik[47] and Clegg and Brimblecombe.[48] In many nucleation studies in the literature Eq. (20) is considered to give the total rather than the free acid concentration and pressure. Expression (13) is then applied to obtain the free acid concentration needed in the nucleation calculations [see, for example, Eqs. (11) and (28)].[26] This approach would be correct if the activities were obtained by the measurements of total acid pressure (free acid molecules plus hydrates) in the equilibrium vapor above acid solutions. The data of sulfuric acid activity commonly used in nucleation calculations (e.g., activities by Zeleznik[47] and Clegg and Brimblecombe[48]) have been obtained by measurements related to the number concentration or the pressure of free acid molecules, not to the total acid concentration.[46] Therefore, Eq. (20) is valid directly for the free acid pressure.

The equilibrium vapor pressure of pure water (Preining *et al.*[52]) is considered to be known accurately. The equilib-

rium vapor pressure of pure acid by Ayers *et al.*[53] corrected by Kulmala and Laaksonen[54] is given by

$$p_a^{\mathrm{pure}}/\mathrm{atm} = \exp\left\{ L + 10156\left[\frac{1}{360.15} - \frac{1}{T} + \frac{0.38}{545} \times \left(1 + \ln\left(\frac{360.15}{T} \right) - \frac{360.15}{T} \right) \right] \right\}, \quad (21)$$

where $L=-11.94$. In the following calculations also the parameter L is submitted to fitting. The range of temperature in the experiments by Marti *et al.*[39] was narrow, only 10 K. It is therefore not reasonable to submit the parameter represented by the value of 10156 (enthalpy of vaporization divided by the molar gas constant R) to the fitting.

Numerical estimation shows that the sum in Eq. (13) is dominated by three first terms. To take approximately into account the very weak effect of larger hydrates the enthalpies and entropies for $i=3$, 4, and 5 were calculated using the classical droplet model [Eq. (15)] with mole fraction x_{ave} [Eq. (16)] at $T=298.15$ K. Equation (15) was preferred over more correct Eq. (17) because the enthalpy and entropy values obtained in this way were closer to the *ab initio* values. The same reason led us to choose the less accurate approximation for the hydrate composition. As Fig. 2 shows, the relative importance of the larger hydrates is rather small, and the choice of approximation is insignificant. The differences between nucleation rates calculated with different versions of the classical theory for hydrates containing 3–5 water molecules is negligible.

The formation enthalpies and entropies of mono- and dihydrates are used as fitting parameters. The results of *ab initio* calculations by Bandy and Ianny[55] show that when decreasing temperature from $T=298$ K the enthalpy ΔH_1 and entropies of hydration ΔS_i $(i=1,2)$ will first grow a little. At the temperature $T=223$ K the entropies ΔS_1, ΔS_2 are 0.3% and 0.2% higher, respectively, than at room temperature. The difference for the enthalpy ΔH_1 is 1%. The enthalpy ΔH_2 is 0.3% larger at this temperature. After the temperature value of about 223 K the enthalpy ΔH_1 and entropies of hydration ΔS_1, ΔS_2 will diminish regaining approximately their initial values at $T=173$ K. The enthalpy ΔH_2 increases in this temperature interval reaching the value which is at $T=173$ K 1% larger than the initial values at $T=298$ K. Also the change in values of larger hydrates is small (smaller than 2.3%). Based on these results the temperature dependence of the enthalpies and entropies of hydration was ignored in this study.

The fitting was performed by finding the minimum of the sum,

$$S = \frac{\sum_{i=1}^{54}[Y_i - y_i(\Delta H_1, \Delta S_1, \Delta H_2, \Delta S_2, L)]^2}{2\sigma_i^2}, \quad (22)$$

where Y_i is the known value obtained from the measurements/*ab initio* calculations, $y_i(\Delta H_1, \Delta S_1, \Delta H_2, \Delta S_2, L)$ is the theoretical value, which depends on the fitting parameters, and σ_i is the estimated standard deviation of the known value.

Marti *et al.*[39] estimated the composition uncertainty of solutions in their experiments to be 15% and the uncertainty of obtained total vapor pressures of acid to be 36%. Due to a steep dependence of activity A_a on composition x the uncertainty of 15% gives rises to the uncertainties of acid pressure of 1500–8300%. It is therefore appropriate to choose $Y_{i=1,\ldots,47}=x_{\mathrm{mass},i}$ where $x_{\mathrm{mass},i}$ is the mass fraction of the data point i and $y_{i=1,\ldots,47}=x_{\mathrm{mass}}(p_{a,i}^{\mathrm{total}})$ is the mass fraction that satisfies Eqs. (13) and (20) for $\rho_a^{\mathrm{total}}=p_{a,i}^{\mathrm{total}}/kT$, where $p_{a,i}^{\mathrm{total}}$ is the experimental value. The estimate $\sigma_{i=1,\ldots,47}=0.014$ for standard error of $x_{\mathrm{mass},i}$ is taken from Noppel.[27]

Hanson and Eisele[51] measured the wall loss of sulfuric acid vapor as a function of relative humidity and obtained the values $K_1=410\pm94.5$ and $K_2=50\pm9.45$ for the equilibrium constants of hydrate formation (precision of two standard deviations). The equilibrium constants are dimensionless, the reference pressure is 1 atm. These results are represented by the two terms with

$$y_{48,49} = \exp\left(\frac{\Delta H_{1,2} - T\Delta S_{1,2}}{RT} \right) \quad (23)$$

and $Y_{48}=410$ $Y_{49}=50$, $\sigma_{48}=94.5/2$, $\sigma_{49}=9.45/2$ in the sum S.

The *ab initio* values obtained by Re *et al.* with the D95++(d,p) basis set were considered to be the most accurate. The average of enthalpy changes for the monohydrate I-n and I-c structures, $Y_{50}=-41.2$ kJ/mol, is considered as an average value for ΔH_1. The standard deviation of ΔH_1 is taken to be 21 kJ/mol, which is the approximate variation range of *ab initio* values given in Table I. Accordingly, the estimate for ΔS_1 is $Y_{51}=-121$ J/(mol K) and the standard deviation is 8.3 J/mol. For dihydrate the enthalpy values of II-n-a and II-n-b structures were used. The average value for ΔH_2 was taken to be $Y_{52}=-45.6$ kJ/mol and for ΔS_2 the average is $Y_{53}=-130$ J/(mol K). The values of standard deviations for ΔH_2 and ΔS_2 were taken to be the same as for the monohydrate. This added four more terms with $y_{50,51}=\Delta H_{1,2}$, $y_{52,53}=\Delta S_{1,2}$, $\sigma_{50,51}=8.3$ J/mol, and $\sigma_{52,53}=21$ kJ/(mol K) to the sum.

The final term $Y_{54}=-11.94$ and $y_{54}=L$ arises from the parameter L in the saturation vapor pressure of pure sulfuric acid [Eq. (21)]. The standard deviation of L is taken to be $\sigma_{54}=0.437/2$, since 0.437 is the estimated measurement error by Ayers *et al.*[53]

The result obtained when applying the activities by Zeleznik[47] are presented in the first column of Table II. We also present the equilibrium constants that were used for larger hydrates. The value of $K_1=558$ calculated at $T=298.15$ deviates clearly from the experimental value 410,[51] the difference being around three standard deviations. The value of $K_2=53.8$ at $T=298.15$ is well within the range of experimental errors, 50 ± 9.45. The same is true for the parameter L (experimental value -11.94 ± 0.437). The value -$\Delta H_1=51.21$ kJ/mol is 9.3% larger than the value of I-n structure by Re *et al.* [(D95++(d,p) basis set] which should be the most realistic structure. The obtained entropy value is 3% larger than the value of I-n structure. As with classical droplet model, the values for dihydrates show better

TABLE II. Gas phase hydration enthalpies ΔH_i, entropies ΔS_i, free energies ΔG_i, $(i=1,2)$ and equilibrium constants K_i $(i=3,4,5)$ and the parameter L related to the pure sulfuric acid vapor pressure, Eq. (21). The equilibrium constants are calculated at reference pressure 1 atm. The values in this table result from the fitting procedure described in Sec. IV. We compare the values obtained with Zeleznik (Ref. 47) and Clegg *et al.* activities.

Zeleznik activities	Clegg and Brimblecombe activities
$\Delta H_1=-51.21$ kJ/mol	$\Delta H_1=-51.02$ kJ/mol
$\Delta S_1=-119.2$ J/(mol K)	$\Delta S_1=-119.2$ J/(mol K)
$\Delta H_2=-48.34$ kJ/mol	$\Delta H_2=-48.31$ kJ/mol
$\Delta S_2=-129.0$ J/(mol K)	$\Delta S_2=-129.0$ J/(mol K)
$L=-11.695$	$L=-11.387$
$K_3=\exp(5246/T-14.90)$	$K_3=\exp(4430/T-12.14)$
$K_4=\exp(4934/T-14.47)$	$K_4=\exp(4384/T-12.60)$
$K_5=\exp(4763/T-14.21)$	$K_5=\exp(4371/T-12.87)$

agreement with *ab initio* values. The values for ΔH_2 and ΔS_2 differ 2.2% and 1.6% from the II-n-a structure, respectively.

The model by Clegg and Brimblecombe[48] gives the activity of sulfuric acid in aqueous solutions with respect to the reference state of infinite dilution of sulfuric acid. To obtain activity values for the reference state of pure liquid we divided their activity values $A_a=(x_{\mathrm{H}}f_{\mathrm{H}})^2x_{\mathrm{SO_4}}f_{\mathrm{SO_4}}$ by their activity values at pure liquid acid (in practice pure acid was represented by a solution with molality 10^7 mol/kg corresponding to mole fraction 0.999 995). Here x_{H}, $x_{\mathrm{SO_4}}$ are the mole fractions and f_{H}, $f_{\mathrm{SO_4}}$ are the activity coefficients of ions H^+ and SO_4^{2-} in the solution, respectively. The activity values for pure liquid acid are out of applicability range of the model by Clegg and Brimblecombe which is 0–40 mol/kg (corresponding to mole fractions 0–0.41). So some uncertainty is introduced into the activities, and it cannot be separated from the uncertainty of the pure acid saturation vapor pressure. For this reason the last term with $i=54$ was removed from the sum to be minimized when using Clegg and Brimblecombe activities. The values for fitted parameters are presented in the second column of Table II. They are very close to the values obtained when using activities by Zeleznik.[47] The results of the fitting are now applied to nucleation rate calculations.

V. SELF-CONSISTENT EQUILIBRIUM BINARY DISTRIBUTION

Wilemski[56] has shown that commonly used cluster size distribution introduced by Reiss,[23]

$$\rho(n_a,n_w)=(\rho_a^{\mathrm{tot}}+\rho_w^{\mathrm{tot}})\exp\left(-\frac{\Delta G(n_a,n_w)}{kT}\right) \tag{24}$$

does not obey the law of mass action.

For a vapor regarded as an ideal gas mixture the number density of clusters containing n_a and n_w acid and water molecules, respectively, can be expressed by the law of mass action,

$$\rho(n_a,n_w)=K(\rho_a^{\mathrm{free}})^{n_a}(\rho_w^{\mathrm{free}})^{n_w}, \tag{25}$$

where K is an equilibrium constant which does not depend on water and acid concentrations in the vapor. The equilibrium distribution (24) by Reiss can be expressed as

$$\rho(n_a,n_w)=K(\rho_a^{\mathrm{free}})^{n_a}(\rho_w^{\mathrm{free}})^{n_w+1}, \tag{26}$$

where K does not depend on water and acid vapor pressures and the concentrations of water vapor is considered to be much larger than that of acid. We see that the equilibrium distribution by Reiss gives a stronger dependence of the number concentration of clusters on the vapor pressure of water and consequently the nucleation rate is also a steeper function of relative humidity. One form of equilibrium distribution that obeys the law of mass action is given by the expression[57]

$$\rho(n_a,n_w)=\rho_a^{\mathrm{free}}\left(\frac{\rho_w^{\mathrm{free}}}{\rho_0}\right)^2K_1K_2\times\exp\left(-\frac{\Delta G(n_a,n_w)-\Delta G(1,2)}{kT}\right), \tag{27}$$

where $\Delta G(1,2)$ is the formation work of the sulfuric acid dihydrate according to the classical liquid drop model [Eq. (11)]. Note that evaluation of the classical formation free energy of the hydrate requires solving the core composition as explained below Eq. (16). Distribution (27) is a generalization of Eq. (12) and it is adjusted so that it gives a dihydrate concentration equal to the one given by Eq. (12). Any other cluster size for which the equilibrium constant (or formation free energy, enthalpy and entropy) are known from experiments or *ab initio* calculations could alternatively be chosen as the reference size.

VI. WORK OF FORMATION OF THE CRITICAL CLUSTER

For the critical cluster the work of formation corresponds to the saddle point of the free energy surface given by Eq. (11). The critical cluster can be identified by finding the minimum of the formation free energy with respect to n_a and n_w. The derivatives are taken in the similar manner as in deriving Eq. (15) (see Laaksonen *et al.*[43] for details). This leads to the equation

$$v_w(x^*)\ln\frac{\rho_a^{\mathrm{free}}}{\rho_{a,s}^{\mathrm{free}}(x^*)}=v_a(x^*)\ln\frac{\rho_w^{\mathrm{free}}}{\rho_{w,s}^{\mathrm{free}}(x^*)} \tag{28}$$

which determines the critical cluster composition x^*. The asterisk refers to the critical cluster. The radius of the critical cluster is then given by the Kelvin equation,

$$r^*=\frac{2\gamma(x^*)v_i(x^*)}{kT\ln(\rho_i^{\mathrm{free}}/\rho_{i,s}^{\mathrm{free}}(x^*))}, \tag{29}$$

where Eq. (28) ensures that the value of r^* is independent of the choice of the component $i=a,w$.

The work of formation for the critical nucleus is

$$W^*=\tfrac{4}{3}\pi r^{*2}\gamma(x^*). \tag{30}$$

VII. NUCLEATION RATE

The general expression for nucleation rate J is[58,59]

$$J=\frac{|\lambda|/\pi}{\sqrt{-\det(\mathbf{D}/\pi)}}\rho(n_a^*,n_w^*), \tag{31}$$

where $\rho(n_a^*,n_w^*)$ is the number density of critical clusters. The elements of matrix **D** are given by

$$D_{ij}=\frac{1}{2kT}\frac{\partial^2 W(n_a,n_w)}{\partial n_i \partial n_j}\bigg|_{n_a^*,n_w^*}, \tag{32}$$

where $i,j=a,w$. λ is the negative eigenvalue of the product matrix **KD**, and **K** is the growth tensor with elements,

$$K_{aa}=\sum_{n_a',n_w'}^{\xi} n_a' n_a' k(n_a',n_w';n_a^*,n_w^*)\rho(n_a',n_w'), \tag{33}$$

$$K_{wa}=\sum_{n_a',n_w'}^{\xi} n_a' n_w' k(n_a',n_w';n_a^*,n_w^*)\rho(n_a',n_w')=K_{aw} \tag{34}$$

$$K_{ww}=\sum_{n_a',n_w'}^{\xi} n_w' n_w' k(n_a',n_w';n_a^*,n_w^*)\rho(n_a',n_w'). \tag{35}$$

The sums represent clusters of size n_a',n_w' colliding with the critical cluster. The collision probability is

$$k(n_a',n_w';n_a^*,n_w^*)=(r^*+r')^2\sqrt{8\pi kT\left(\frac{1}{m^*}+\frac{1}{m'}\right)}, \tag{36}$$

where m^*, m', r^*, r' are, respectively, the masses and radii of the critical cluster and the cluster colliding with it. ξ represents the cutoff size, above which the concentrations of clusters are so low that their collisions with the nucleating cluster can be ignored. In this work free water ($n_a'=0,n_w'=1$) and free acid molecules ($n_a'=1,n_w'=0$), and also hydrates containing one acid molecule together with up to five water molecules ($n_a'=1,n_w'=1,...,5$) are taken into account.

Equations (28), (29), and (30) give the composition and formation free energy for the critical cluster. We can use Eqs. (4) and (5) for the numbers of molecules in the interior of the cluster n_{il}. We have to calculate the surface excess numbers n_{is} [Eqs. (7) and (8)] to find the total molecular numbers. These are needed for accurate evaluations of the growth tensor (mass of the cluster) and the second derivatives D_{ij} in Eq. (32). Here we also need information about noncritical clusters; taking the derivatives take us from the critical cluster to slightly modified, noncritical clusters. The method for calculating the core composition of these clusters is explained below Eq. (16).

VIII. RESULTS

We performed the nucleation calculations by two computer codes written in Mathcad and FORTRAN90 by two independent persons (M.N. and H.V.). To avoid programming errors we made sure that the results of the two programs agree in all the cases studied. In Fig. 1 the ratio of free acid to total acid concentration is presented. At temperature 298.15 K the differences between calculations with Clegg *et al.*[48] and Zeleznik[47] activities are very small. The differences arise mainly indirectly from the difference in the fitted values presented in Table II. At temperature $T=210.15$ K the difference between curves is slightly increased due to different behavior of the activities. The classical liquid drop model [CLD, Eqs. (14), (15), and (16)] gives significantly different results, especially at low temperatures.

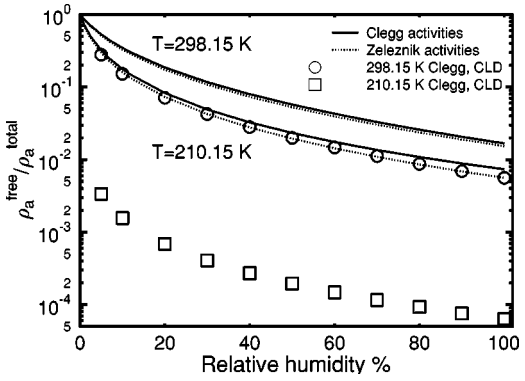

FIG. 1. The ratio of free to total acid concentrations as a function of relative humidity at two different temperatures. The result obtained using the activities by Clegg and Brimblecombe (Ref. 48) and Zeleznik (Ref. 47) are compared. The values calculated by classical liquid drop model (CLD) [Eqs. (14), (15), and (16)] are also shown.

Figure 2 shows the distribution of the hydrates at two different temperatures. Again, the differences between Clegg *et al.* and Zeleznik activities increases slightly at low temperatures, but is not significant. The results of classical droplet model are shown for comparison. The classical model gives a rather good order of magnitude estimates for the hydrates, but the difference in the free acid concentrations shown also in Fig. 1 is significant in the nucleation calculations since these concentrations enter the expression for the formation energy of a cluster. Even though the equilibrium constants for hydrates with $i=3,4,5$ are taken from the classical droplet model, their concentration differs from the clas-

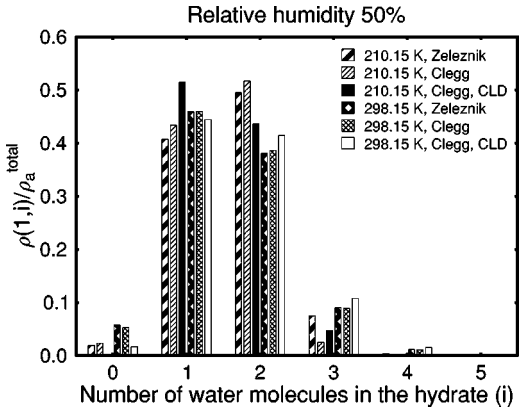

FIG. 2. Size distribution of hydrates of sulfuric acid in the vapor phase at relative humidity 50% at two different temperatures. The result obtained using the activities by Clegg and Brimblecombe (Ref. 48) and Zeleznik (Ref. 47) are compared. The values calculated by classical liquid drop model (CLD) [Eqs. (14), (15), and (16)] are also shown.

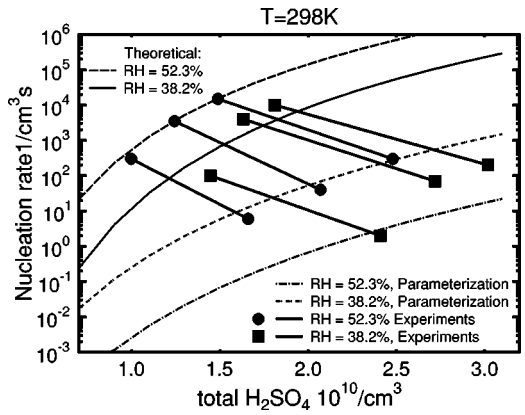

FIG. 3. The nucleation rates at temperature 298.15 K and relative humidities 38.2% and 52.3%. The results are calculated using Clegg *et al.* (Ref. 48) activities and self-consistent size distribution (27). Experimental results of Viisanen *et al.* (Ref. 31) and the parameterization by Kulmala *et al.* (Ref. 30) are shown for comparison.

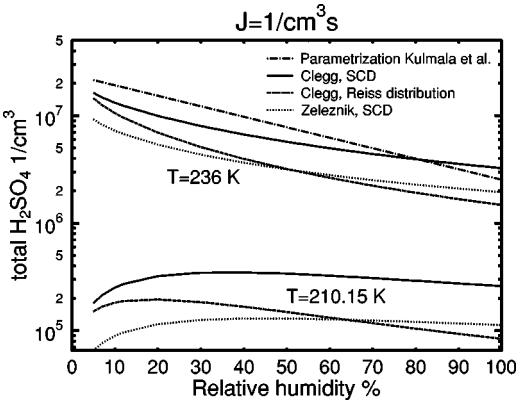

FIG. 4. The onset conditions for nucleation at temperatures 210.15 K and 236 K. The results of calculations with Zeleznik (Ref. 47) and Clegg *et al.* (Ref. 48) activities are compared. We also compare the results obtained using the Reiss equilibrium distribution presented in Eq. (24) and the self-consistent distribution (SCD) of Eq. (27). At 236 K the parameterization of Kulmala *et al.* (Ref. 30) is also shown for comparison.

sical value since it depends also on the equilibrium constants K_1 and K_2 according to Eq. (12).

Figure 3 shows the nucleation rates at 298 K as a function of total sulfuric acid concentration in the vapor at two relative humidities 38.2% and 52.3%. Viisanen *et al.*[31] measured the binary nucleation rate at these relative humidities. In their experiments the sulfuric acid concentration and nucleation time were uncertain. The uncertainty in the experimental results are represented by lines: One end lies at the maximum sulfuric acid concentration value and the maximum nucleation time 50 s given by Viisanen *et al.*, and the other end at minimum sulfuric acid concentration (0.6 times the maximum) and minimum nucleation time 1 s. The higher nucleation rate end of the experimental range agrees nicely with the theoretical predictions within one order of magnitude. The experimental point with relative humidity 52.3% and sulfuric acid concentration $1.25 \cdot 10^{10}$ cm^{-3} is left out since at that point the measured nucleation rate is very uncertain. We also compare our results with the parameterization by Kulmala *et al.*[30] The nucleation rates given by the parameterization are considerably lower than the ones given by the present model. Note also that the dependence on sulfuric acid concentrations (slopes of the curves differ between the models) as well as relative humidity (the present model curves lie closer together than the parameterization curves) is different between the models. Especially at relative humidity 52.3% the slope of our theoretical curve agrees almost exactly with the experimental results.

Figure 4 show onset conditions for nucleation rate $J = 1/\mathrm{cm}^3\,\mathrm{s}$ at temperatures 236 K and 210.15 K. We compare results obtained using Clegg *et al.* and Zeleznik activities. Also the effect of the equilibrium distribution is shown. Reiss distribution (24) gives a stronger relative humidity dependence than the self-consistent distribution given by Eq. (27). We also tested another form for the self-consistent distribution suggested by Wilemski and Wyslouzil.[56] The results did not change significantly if their distribution was adjusted to give the same value for the concentration of dihydrates as Eqs. (12) and (27). If we chose monohydrate instead of dihydrate as the reference size in Eq. (27) our results did not change significantly. We also compare our results with the earlier parameterization at 236 K. The parameterization is not valid at 210.15 K.

Figure 5 shows the onset conditions for nucleation rate $J = 10^7/\mathrm{cm}^3\,\mathrm{s}$ at 236 K using different activities and equilibrium distributions. The experimental result by Eisele and Hanson[40] and the parameterization of Kulmala *et al.*[30] are also shown. The present theory seems to underestimate the amount of sulfuric acid needed for nucleation, in other words the theory overestimates the nucleation rate compared to experiments.

In Figs. 4 and 5 the amount of sulfuric acid required for nucleation increases with relative humidity in some cases. This might seem nonphysical at first glance, but can be explained as follows: When the relative humidity increases the concentration of free sulfuric acid molecules decreases due to strong hydrate formation. The free acid concentration is the one that enters the energetics of the cluster formation

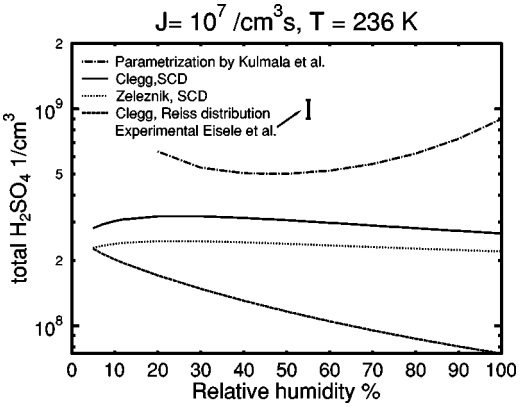

FIG. 5. The conditions for nucleation rate $J = 10^7/\mathrm{cm}^3\,\mathrm{s}$ at 236 K. The results of calculations with Zeleznik (Ref. 47) and Clegg *et al.* (Ref. 48) activities are compared. We also compare the results obtained using the Reiss equilibrium distribution presented in Eq. (24) and the self-consistent distribution (SCD) of Eq. (27). The experimental data point of Eisele *et al.* (Ref. 40) and the parameterization by Kulmala *et al.*[30] are shown for comparison.

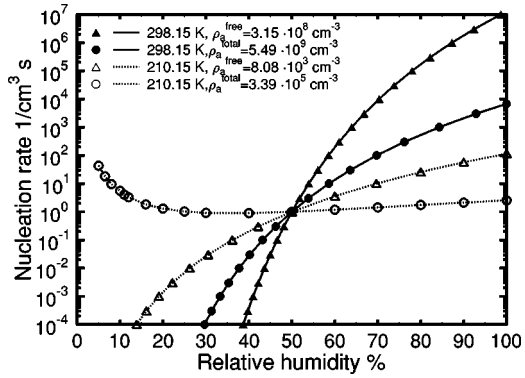

FIG. 6. Nucleation rate dependence on relative humidity at temperatures 210.15 K and 298.15 K. The behavior with constant total concentration of sulfuric acid and constant concentration of free sulfuric acid are compared. All results are calculated using Clegg *et al.* (Ref. 48) activities and the self-consistent distribution (27).

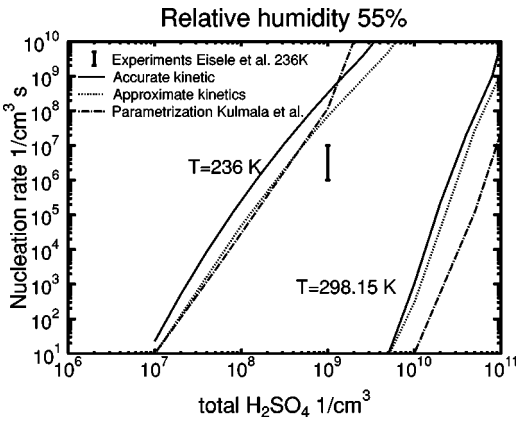

FIG. 7. Nucleation rate dependence on total concentration of sulfuric acid at temperatures 236 K and 298.15 K. All results are calculated with Clegg activities (Ref. 48) and the self-consistent distribution [Eq. (27)]. The experimental data of Eisele *et al.* (Ref. 40) the parameterization by Kulmala *et al.* (Ref. 30) are shown for comparison.

(11) and determines the nucleation rate. Figure 6 clarifies this point: we have compared the nucleation rates with constant free acid concentration and constant total acid concentration at two different temperatures. The values for acid concentrations have been chosen so that we get nucleation rate $J = 1/\mathrm{cm}^3\,\mathrm{s}$ at relative humidity 50% in all the cases. The constant free acid concentration curves behave as expected: the nucleation rate grows monotonously with relative humidity. At the low temperature and low relative humidities the curves with constant total acid concentration show a decrease in nucleation rate with increasing relative humidity.

The model behind the Kulmala *et al.*[30] parameterization uses the equilibrium distribution by Reiss and activities by Taleb *et al.*[60] The hydrates were treated according to the classical droplet model, and the activities are considered to give the total rather than the free acid concentration [see Eq. (20) and text below]. The partial molar volumes were set constant in their calculations, and the kinetics was treated approximately using the concept of virtual monomer and steepest descent approximation.[61] This approximation avoids evaluation of the second derivatives in Eq. (32), and the effect of surface excess molecules is ignored. Also all other terms but those corresponding to free sulfuric acid and water molecules were missing in the diagonal terms of the growth tensor, Eqs. (33) and (35). This results in 1–3 orders of magnitude too low nucleation rates depending on the degree of hydrate formation. It must be kept in mind that the nucleation rate parameterization of Kulmala *et al.*[30] does not agree exactly with their model calculations, but rather provides an order of magnitude estimate for atmospheric models. For example the lack of curvature in the line representing the parameterization in Fig. 4 is probably due to the crudeness of the parameterization.

In Fig. 7 we compare the nucleation rates of this work with the parameterization at 236 K and 298.15 K. The experimental point of Eisele and Hanson[40] is again shown. We also indicate the effect of approximate kinetics[30] [without the mistake in Eqs. (33) and (35)]. At 236 K the kinetics alone is enough the explain the difference between the models, but at higher temperatures other effects are significant. We also tested the effect of surface excess molecules: using the average liquid mole fraction (16) when evaluating the derivatives in Eq. (32) and also the core molecular numbers n_{il} as the total numbers n_i when evaluating the mass of the critical cluster does not change the results when the critical cluster is larger than about ten molecules. For example the inaccuracy in the mass of the cluster is less than 2.5%. With smaller clusters, however, the accurate description of the kinetics is not possible without the surface excess correction since the determinant in the denominator of nucleation rate (31) turns positive and the square root imaginary.

Figure 8 compares the nucleation rates given by our calculations with the experimental results of Ball *et al.*[34] In the experiments of Ball *et al.* the sulfuric acid concentration in the nucleation zone is estimated to be around 7.3–66 (22%–67%/+200%) times larger than the one measured at the end of chamber. The uncertainty of this factor means that the measured dependence of nucleation rate on the acid concentration is an estimate. The theoretical nucleation rates are

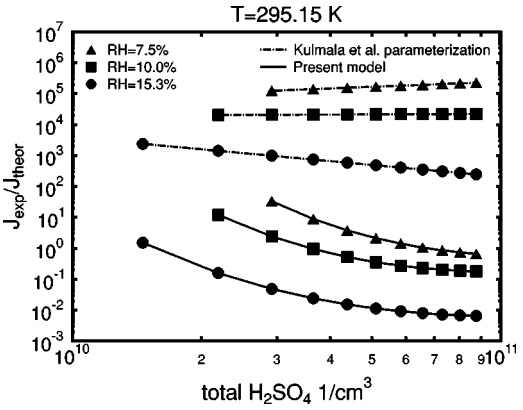

FIG. 8. Experimental nucleation rate divided by the theoretical prediction as a function of total concentration of sulfuric acid at different values of relative humidity at 295.15 K. Theoretical results are calculated using Clegg *et al.* (Ref. 48) activities and the self-consistent distribution [Eq. (27)]. Experimental rates are calculated from the data of Ball *et al.* (Ref. 34) assuming that the sulfuric acid concentration at the nucleation zone is 7.3 times higher than at the end of their chamber (their lower limit). We also show a comparison to the parameterization of Kulmala *et al.* (Ref. 30).

within two orders of magnitude compared to the experimental ones if the lower limit of uncertainty (factor 7.3) is used. We also have compared the parameterization of Kulmala *et al.*[30] with the experimental results. With factor 7.3 the nucleation rates given by the present model lie closer to the experimental points than the parameterization results, but the sulfuric acid dependence of the parameterization agrees better with the experiments (the parameterization lines are almost horizontal). Both models produce quite a similar relative humidity dependence (separation of the curves). For example with factor 22 the situation is quite different: the present model gives clearly better relative humidity dependence, but the nucleation rates are further from the experimental values compared to the parameterization. In this case there is no significant difference in the dependence on acid concentration between the models. We have left experiments with relative humidities 2.3%, 4.6%, and 4.8% out from Fig. 8, since the nucleation rate at most of these points is very low, and the theoretical rates can differ from the experimental ones by several orders of magnitude. In this region the predictions of the theory are inaccurate since the numerical errors are of the same order of magnitude as the results. Furthermore, for low relative humidities the theoretical critical cluster composition is close to the upper limit of the region where Clegg *et al.* activities can be used. Also the inaccuracy of the experiments might be emphasized in the case of low nucleation rates.

IX. CONCLUSIONS

In this paper the hydrate formation in the water-sulfuric acid vapor is investigated. The different approximations used in the classical droplet model will cause differences in the equilibrium constants of hydrate formation. On the other hand the nucleation rate is rather sensitive to the equilibrium constants. We have therefore developed a more reliable model for the hydrate formation. Our estimates are based on *ab initio* structures of small water–sulfuric acid clusters and on experimental results for equilibrium constants and equilibrium vapor pressures. In this paper we report new, improved values for the formation enthalpies, entropies, and equilibrium constants for sulfuric acid mono- and dihydrates. We have tested the sensitivity of the fitting procedure (see also recent work by Noppel[27]) and found that it is very stable against small changes in the experimental and *ab initio* values it is based on. Compared to the most commonly used classical droplet model,[26] the vapor phase concentrations of the free acid molecules are significantly higher according to the present model. In practice, the free acid concentration determines the formation energy of the nucleating clusters, and therefore affects strongly on the calculated nucleation rates. Our method can be readily extended to take into account further incoming information on the hydrates from new experiments and improved computer simulations, which are likely to improve our picture of small molecular clusters in the future.

In this study two different thermodynamic models for liquid phase activities are compared and the results show that hydration and nucleation rate are not sensitive to the thermodynamic model used. It should be noted that the Clegg *et al.*[48] and Zeleznik[47] activities used in this study give directly the free acid concentrations in the equilibrium vapor rather than the total sulfuric acid concentrations as assumed in several nucleation studies in the literature.

We checked also the effect of differences in the density and surface tension models and found that they do not cause significant changes in the nucleation rates. We have also tested the effect of the equilibrium distribution used on the nucleation rate. A distribution obeying the mass action law gives a weaker dependence of nucleation rate on the relative humidity than the commonly used Reiss distribution.[23]

In this work the nucleation rates have been obtained using the rigorous nucleation kinetics and thermodynamically consistent version of the classical model. The results have been compared with experimental nucleation rates (Viisanen *et al.*, Ball *et al.*[31,34]). In most cases the theoretical values are within experimental area. However, at lower temperatures (Eisele and Hanson[40]) there is some disagreement. The present theory somewhat overestimates the nucleation rate compared to the recent parameterization by Kulmala *et al.*[30] Besides relying to the classical model for hydrates and the Reiss equilibrium distribution,[23] the model behind the parameterization contains several approximations and the kinetic part is partly erroneous. These factors explain the discrepancy between the parameterization and the present results.

The nucleation theorems[62,63] indicate that besides the absolute values of the nucleation rate also the slopes of the nucleation rate curves plotted against the acid concentration and the relative humidity are fundamentally important. The slopes are directly connected to the size and formation energy of the nucleating clusters. The self-consistent equilibrium distribution and the new description of hydrate formation change the slopes of the nucleation rate. The slopes given by the present theory agree well with the experimental results of Viisanen *et al.*, but the analysis of the measurements of Ball *et al.* is ambiguous. The compatibility depends strongly on the estimate for the sulfuric acid concentration in the nucleation zone. More accurate measurements are pressingly needed to determine how well the classical theory really works for sulfuric acid–water nucleation.

ACKNOWLEDGMENTS

This work was supported by Maj and Nessling Foundation, the Estonian Science Foundation (Grant No. 3903) and Academy of Finland (Project No. 48984).

[1] R. J. Charlson and T. Wigley, Sci. Am. **270**, 48 (1994).
[2] D. W. Dockery and C. Pope, Annu. Rev. Public Health **15**, 107 (1994).
[3] A. Clarke, J. Atmos. Chem. **14**, 479 (1992).
[4] F. Schröder and J. Ström, J. Atmos. Res. **44**, 333 (1997).
[5] F. Raes *et al.*, J. Geophys. Res., [Atmos.] **102**, 21315 (1997).
[6] D. S. Covert, V. N. Kapustin, P. K. Quinn, and T. S. Bates, J. Geophys. Res., [Atmos.] **97**, 20581 (1992).
[7] W. A. Hoppel, G. M. Frick, J. W. Fitzgerald, and R. E. Larson, J. Geophys. Res., [Atmos.] **99**, 14443 (1994).
[8] C. O'Dowd *et al.*, Geophys. Res. Lett. **25**, 1661 (1998).
[9] D. Hegg, L. Radke, and P. Hobbs, J. Geophys. Res., [Atmos.] **96**, 18727 (1991).
[10] A. Wiedensohler *et al.*, Tellus, Ser. B **48B**, 213 (1996).

[11] L. Pirjola, A. Laaksonen, P. Aalto, and M. Kulmala, J. Geophys. Res., [Atmos.] **103**, 8309 (1998).
[12] V.-M. Kerminen and A. Wexler, Tellus, Ser. B **48B**, 65 (1996).
[13] J. M. Mäkelä *et al.*, Geophys. Res. Lett. **24**, 1219 (1997).
[14] M. Kulmala *et al.*, Tellus, Ser. B **53**, 324 (2001).
[15] I. Kavouras, N. Mihalopoulos, and E. Stephanou, Nature (London) **395**, 686 (1998).
[16] A. Laaksonen and D. W. Oxtoby, J. Chem. Phys. **102**, 5803 (1995).
[17] H. Arstila, K. Laasonen, and A. Laaksonen, J. Chem. Phys. **108**, 1031 (1998).
[18] I. Kusaka, Z.-G. Wang, and J. H. Seinfeld, J. Chem. Phys. **108**, 6829 (1998).
[19] J. H. Seinfeld and S. N. Pandis, *Atmospheric Chemistry and Physics: From Air Pollution to Climate Change* (Wiley, New York, 1998).
[20] P. Korhonen, M. Kulmala, and Y. Viisanen, J. Aerosol Sci. **28**, 901 (1997).
[21] S. L. Clegg, P. Brimblecombe, and A. S. Wexler, J. Phys. Chem. A **102**, 2137 (1998).
[22] H. Flood, Z. Phys. Chem. Abt. A **170**, 286 (1934).
[23] H. Reiss, J. Chem. Phys. **18**, 840 (1950).
[24] G. J. Doyle, J. Chem. Phys. **35**, 795 (1961).
[25] R. H. Heist and H. Reiss, J. Chem. Phys. **61**, 573 (1974).
[26] A. Jaecker-Voirol, P. Mirabel, and H. Reiss, J. Chem. Phys. **87**, 4849 (1987).
[27] M. Noppel, J. Geophys. Res., [Atmos.] **105**, 19779 (2000).
[28] G. Wilemski, J. Chem. Phys. **80**, 1370 (1984).
[29] A. Laaksonen, M. Kulmala, and P. E. Wagner, J. Chem. Phys. **99**, 6832 (1993).
[30] M. Kulmala, A. Laaksonen, and L. Pirjola, J. Geophys. Res., [Atmos.] **103**, 8301 (1998).
[31] Y. Viisanen, M. Kulmala, and A. Laaksonen, J. Chem. Phys. **107**, 920 (1997).
[32] P. Mirabel and J. Clavelin, J. Chem. Phys. **68**, 5020 (1978).
[33] B. E. Wyslouzil, J. H. Seinfield, and R. C. Flagan, J. Chem. Phys. **94**, 6827 (1991).
[34] S. M. Ball, D. R. Hanson, and F. L. Eisele, J. Geophys. Res., [Atmos.] **104**, 23709 (1999).
[35] R. J. Weber *et al.*, Chem. Eng. Commun. **151**, 53 (1996).
[36] P. Korhonen *et al.*, J. Geophys. Res., [Atmos.] **104**, 26349 (1999).
[37] M. Kulmala, L. Pirjola, and J. M. Mäkelä, Nature (London) **404**, 66 (2000).
[38] R. McGraw and R. J. Weber, Geophys. Res. Lett. **25**, 3143 (1998).
[39] J. Marti *et al.*, J. Geophys. Res., [Atmos.] **102**, 3725 (1997).
[40] F. L. Eisele and D. R. Hanson, J. Phys. Chem. A **104**, 830 (2000).
[41] K. Nishioka and I. Kusaka, J. Chem. Phys. **96**, 5370 (1992).
[42] S. Ono and S. Kondo, in *Encyclopedia of Physics*, edited by S. Flugge (Springer, Berlin, 1960), p. 134.
[43] A. Laaksonen, R. McGraw, and H. Vehkamäki, J. Chem. Phys. **111**, 2019 (1999).
[44] P. Debenedetti, *Metastable Liquids: Concepts and Principles* (Princeton University Press, Princeton, 1996).
[45] R. Alberty, *Physical Chemistry*, 6th ed. (Wiley, New York, 1983).
[46] M. Noppel, J. Chem. Phys. **109**, 9052 (1998).
[47] F. J. Zeleznik, J. Phys. Chem. Ref. Data **20**, 1157 (1991).
[48] S. L. Clegg, J. Chem. Eng. Data **40**, 43 (1995).
[49] C. E. L. Myhre, C. J. Nielsen, and O. W. Saastad, J. Chem. Eng. Data **43**, 617 (1998).
[50] M. Noppel, J. Aerosol Sci. **29**, S377 (1998).
[51] D. Hanson and F. Eisele, J. Phys. Chem. **104**, 1715 (2000).
[52] O. Preining, P. E. Wagner, F. G. Pohl, and W. Szymanski, *Heterogeneous Nucleation and Droplet Growth* (University of Vienna, Institute of Experimental Physics, Vienna, Austria, 1981).
[53] G. P. Ayers, R. W. Gillett, and G. L. Gras, Geophys. Res. Lett. **7**, 433 (1980).
[54] M. Kulmala and A. Laaksonen, J. Chem. Phys. **93**, 696 (1990).
[55] A. R. Bandy and J. C. Ianni, J. Phys. Chem. **102**, 6533 (1998).
[56] G. Wilemski and B. E. Wyslouzil, J. Chem. Phys. **103**, 1127 (1995).
[57] M. Noppel, in *Nucleation and Atmospheric Aerosols 2000, 15th International Conference*, edited by B. Hale and M. Kulmala, AIP Conf. Proc. **534**, 339–342 (AIP, Melville, New York, 2000).
[58] H. Trinkhaus, Phys. Rev. B **27**, 7372 (1983).
[59] H. Arstila, P. Korhonen, and M. Kulmala, J. Aerosol Sci. **30**, 131 (1999).
[60] D.-E. Taleb, J.-L. Ponche, and P. Mirabel, J. Geophys. Res., [Atmos.] **101**, 25967 (1996).
[61] M. Kulmala and Y. Viisanen, J. Aerosol Sci. **22**, S97 (1991).
[62] D. W. Oxtoby and D. Kashchiev, J. Chem. Phys. **100**, 7665 (1994).
[63] I. J. Ford, J. Chem. Phys. **105**, 8324 (1996).
[64] S. Re, Y. Osamura, and K. Morokuma, J. Phys. Chem. A **103**, 3535 (1999).
[65] P. Beichert and O. Schrems, J. Phys. Chem. A **102**, 10540 (1998).
[66] L. Kurdi and E. Kochanski, Chem. Phys. Lett. **158**, 111 (1989).